Asian Journal of Chemistry; Vol. 34, No. 6 (2022), 1543-1548

ASIAN JOURNAL OF CHEMISTRY

https://doi.org/10.14233/ajchem.2022.23702

One-Pot Green Synthesis of Cyclohepta[*d*]pyrimidine-2(5*H*)-thione Derivatives using Iron Titanate ($FeTiO_3$, Ilmenite) Nanoparticles and Evaluation of their Antibacterial Activity

T. RAMBABU*, S. PAUL DOUGLAS and B. VENKATESWARA RAO

Department of Engineering Chemistry, AU College of Engineering (A), Andhra University, Visakhapatnam-530003, India

*Corresponding author: E-mail: chemistryrambabu@gmail.com

Received: 30 December 2021; *Accepted*: 22 March 2022; *Published online*: 18 May 2022; AJC-20820

Iron titanate nanoparticles ($FeTiO_3$-NPs, TiFe-0.5, TiFe-1.0, TiFe-2.0 with fixed and variable compositions of Fe and Ti, respectively) were synthesized under ultrasonication and characterized using XRD, FESEM-EDAX and UV-vis DRS spectral techniques. The XRD analysis has clearly indicated the characteristic peaks in the nanoparticles. The morphologies have shown the spherical shaped particles and in the EDAX analysis, the respective elements (Fe, Ti, O) in the prepared nanoparticles were identified. Similarly, the absorption maxima of the nanoparticles have increased with increase in the Ti content between 380-570 nm. Using these nanoparticles, cyclohepta[*d*]pyrimidine-2(5*H*)-thione derivatives (**4a-e**) were synthesized through one-pot approach with cycloheptanone (**1**), some substituted benzaldehyes (**2a-e**) and thiourea (**3**) as the precursors, which was performed under the guidelines of green chemistry. The progress of the reactions were monitored by TLC and the formed derivatives were characterized by using ^{1}H NMR, FTIR and Mass spectral techniques along with the determination of their melting points. The NPs were magnetically separable and with its recycled forms, the reaction was conducted in **3** consecutive cycles and observed that the % yields have not varied much. The antibacterial activity studies were conducted against Gram-negative *Escherichia coli, Klebsiella pneumonia*, Gram-positive *Staphylococcus aurues*, *Bacillus Subtilis* bacteria with the derivatives (**4a-e**). In these studies, almost all the derivatives have shown from moderate to better antibacterial activity.

Keywords: Green synthesis, Pyrimidine derivatives, Iron titanate, Antibacterial activity.

INTRODUCTION

In organic synthesis, multi-component reactions (MCRs) have been creating several organic derivatives through different mechanisms, catalysts, solvents that possess various biological functions [1-6]. In these reactions, Biginelli reaction has been conducted by several researchers in view of its importance in producing organic derivatives with different antimicrobial activities [7,8]. The reaction majorly forms dihyrdopyrimidines using ethyl acetoacetate, aryl halide and urea or thiourea as the precursors [8]. Apart from these regular substrates, various others synthetic routes were also performed. Using tetrachlorosilane in DMF solvent, some aldehydes, β-dicarbonyl compounds, urea/thiourea, a MCRs was conducted to obtain pyrimidine derivatives [9]. 2-Thiopyrimido benzimidazole derivatives were synthesized by the condensation of 4-isothiocyanato-4-methyl-2-pentanone and 3,3′-diaminobenzidine in methanol under refluxing conditions [10]. The pyrimidine derivatives were also synthesized using some amides, activated nitriles with 2-chloropyridine along with trifluoromethane-sulfonic anhydride [11]. In another approach, the pyrimidine-2-thione derivatives were synthesized using condensation of substituted chalcones, thiourea in the presence of KOH and EtOH under ultrasonic conditions [12].

The major drawbacks observed in all the above approaches is that the higher reaction times, lesser to moderate yields, non-recoverability of the catalysts and lack of usage of magnetically separable metal oxides/metal ferrite nanoparticles. These materials possess large surface area, easily recoverable and could perform reaction even after recycling it for 2-3 consecutive runs. In this aspect, metal ferrites of composition $M^{II}Fe_2O_4$ (M = divalent metal ion like Ti, Mn, Co, Ni, Cu, Zn, Cd, Mg *etc*.) have been contributing for the above-mentioned advantages [13-19]. The divalent M^{2+} ion occupies the tetrahedral voids and the trivalent Fe^{3+} ions occupy the octahedral voids in the FCC cubic close packing [20]. These inorganic metal

spinels have been used as heterogeneous catalysts in the field of organic synthesis, photocatalytic decomposition of organic dyes [21]. Unlike these forms of metal ferrites, synthesis of solid phase iron titanates of composition $FeTiO_3$ (Fe^{2+}, Ti^{4+} and O^{2-} ions) have been reported to possess effective magnetic properties [22]. They possess ilmenite phase in their crystal lattice, which are different from the regular ulvospinel $TiFe_2O_4$ forms (band gap = 2.3 eV) [23,24].

On observing the above results, it was planned to synthesize ilmenite $FeTiO_3$ nanoparticles through a facile sol-gel method under ultrasonication. These nanoparticles were synthesized in three combinations with a fixed weight of Fe and variable composition of Ti. It was designed to synthesize various cyclohepta[*d*]pyrimidine-2(5*H*)-thione derivatives which could exhibit some biological functions, catalyzed by the prior formed $FeTiO_3$ nanoparticles under solvent free conditions. The supporting experimental factors like effect of solvent, nanocatalyst composition, comparison with other existing metal ferrites and optimizing the reaction conditions were studied. The antibacterial activity of the synthesized derivatives was investigated using broth dilution method and the results were reported. The synthesis of such pyrimidine-2-thione derivatives using heterogeneous $FeTiO_3$ nanoparticles under solvent free conditions has remained as unperformed reaction pathway and the same was taken as the objective in the present research work.

EXPERIMENTAL

Iron nitrate [$Fe(NO_3)_2{\cdot}9H_2O$], titanium isopropoxide [$Ti(iso\text{-}C_3H_7)_4$], sodium hydroxide and other required precursors, solvents required for the synthesis of $FeTiO_3$ nanoparticles and pyrimidine-2-thione derivatives were procured from Sigma-Aldrich (AR grade). All the chemical were used without further purification.

Characterization: The resulting NPs were characterized using X-Ray Diffractometer (PANanalytical-X' Pert PRO, Japan) at room temperature using Nickel Filter Cu*K*α radiation (λ = 1.54059 Å) over wide range of $10° \leq 2\theta \leq 80°$ with a scanning speed of 2 min^{-1}. The UV-vis diffuse reflectance spectra were recorded using Single Monochromator UV-2600 (optional ISR-2600Plus, λ up to 1400 nm). The morphology of the as-synthesized samples was investigated by field emission scanning electron microscopy (FE-SEM, LEO1550). Melting points of the organic derivatives (**4a-e**) were determined in open glass capillaries on a Stuart SMP30 apparatus and are uncorrected. IR spectra were recorded as KBr pellets on a Shimadzu FTIR 8400S spectrophotometer. ^{1}H NMR (400 MHz) spectra was recorded on a BrukerDPX 400 spectrophotometer using tetramethylsilane (TMS) as internal standard, $CDCl_3$ and DMSO-d_6 as solvents. HRMS spectra were recorded on a XevoQTof mass spectrometer. Elemental analysis was performed on a Perkin CHNS elemental analyzer. Merck pre-coated plates of Silica gel 60 F_{254} were used for the thin layer chromatography (TLC) examination to verify the pureness of the prepared derivatives under ultraviolet light.

Synthesis of $FeTiO_3$ nanoparticles: In the synthesis of $FeTiO_3$ nanoparticles, 5 mL of 0.5 M iron nitrate solution, 2-3 mL of 0.5 M NaOH and x mL of titanium isopropoxide (TIP) (x = 0.5, 1.0, 2.0) were added in three consecutive beakers (100 mL each) and kept under ultrasonication for 40-60 min to achieve uniform mixing of the ingredients. Then, the mixtures kept under heating at around 100-120 ºC to eliminate the impurities and efficient formation of the ferrites and then temperature was brought to near room temperature. The mixtures were centrifuged at around 5000 rpm and the resultant residues were filtered, dried and washed with EtOH:water mixture. The dry powders were calcinated at near 600-700 ºC and labeled as TiFe-0.5, TiFe-1.0 and TiFe-2.0, respectively with respect to the volume of TIP added.

Synthetic protocol to synthesize pyrimidine-2-thione derivatives (4a-e): In a clean round bottom flask, cycloheptanone (**1**) (1 mmol), substituted benzaldehydes (**2a-e**) (1 mmol) and thiourea (**3**) (1 mmol) were taken and optimum amount of $FeTiO_3$ (5 mol% of each NPs) was added under solvent free conditions (neat). All the reaction contents were refluxed for 4 h under stirring at around 50-60 ºC. The progress of the reaction was examined by TLC and on completion of the reaction the flask was brought to near room temperature. The solid derivatives obtained were washed EtOH and recrystallized. The protocol is shown in **Scheme-I**.

4-Phenyl-3,4,5,6,7,8,9-hexahydro-1*H*-cyclohepta[*d*]-pyrimidine-2(5*H*)-thione (4a): Yield: 83%; m.p.: 225-226 ºC; Physical state/colour: Solid/white; IR (KBr, ν_{max}, cm^{-1}): 1615 (C=N *str.*), 1085 (C-N bend), 3167 (N-H *str.*), 1197 (C=S *str.*), 2940, 2854 (Ar C-H *str.*), 704, 774 (Ar C-H bend), 1493 (Ar C-C *str.*), 1615 (C=C *str.* alkene), 1001 (C-H bend, alkene), 3167 (C-H *str.*, alkene); ^{1}H NMR (400 MHz: $CDCl_3$): δ ppm: 2.1 (2H, t), 1.59-1.63 (2H, m), 3.85 (1H, d), 6.87 (1H, d), 7.04

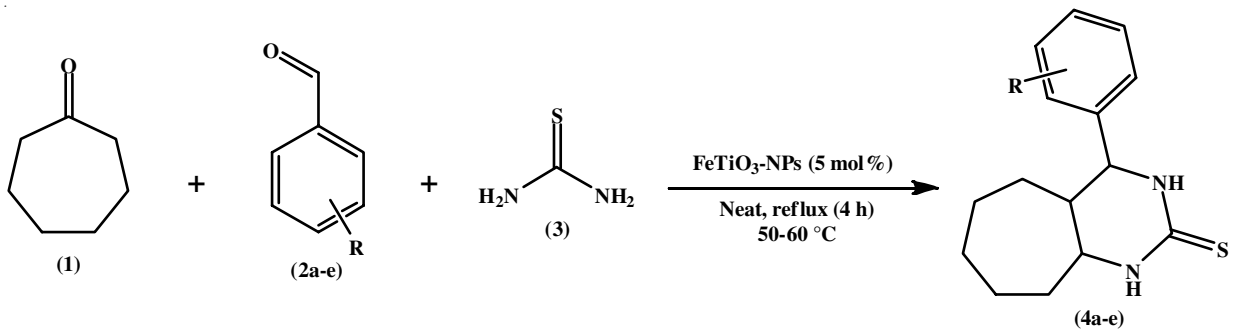

Scheme-I: Synthesis of 4-phenyl-3,4,6,7,8,9-hexahydro-1*H*-cyclohepta[*d*]pyrimidine-2(5*H*)-thione derivatives (**2a**, **4a**: R = H, **2b**, **4b**: R = 4-methoxybenzaldehyde, **2c**, **4c**: R = 3-nitrobenzaldehyde, **2d**, **4d**: R = 6-methoxynapthal, **2e**, **4e**: R = 4-fluorobenzaldehyde

(1H, s), 6.59-7.21 (m, Ar-H, *J* = 2.3 Hz); Mass: $[M+H]^+$; *m/z* 258.32; Elemental analysis: $C_{15}H_{18}N_2S$. calcd. formula weight 258.381; C, 69.6%; H, 6.96%; N, 10.8%; S, 12.3%.

4-(4-Methoxyphenyl)-3,4,5,6,7,8,9-hexahydro-1*H*-cyclohepta[*d*]pyrimidine-2(5*H*)-thione (4b): Yield: 88%; m.p.: 262-263 ºC; Physical state/colour: Solid/white; IR (KBr, ν_{max}, cm^{-1}): 1615 (C=N *str.*), 1085 (C-N bend), 3167 (N-H *str.*), 1197 (C=S *str.*), 2940, 2854 (Ar C-H *str.*), 704, 774 (Ar C-H bend), 1493 (Ar C-C *str.*), 1249 (C-O *str.*, -OMe), 1043 (C-O bend, -OMe), 1615 (C=C *str.* alkene), 1001 (C-H bend, alkene), 3167 (C-H *str.*, alkene); ^{1}H NMR δ ppm: 2.1 (2H, t), 1.59-1.63 (2H, m), 3.61 (1H, d), 6.87 (1H, d), 7.04 (1H, s), 3.72 (methoxy proton, s), 6.81-7.15 (m, Ar-H, *J* = 2.3 Hz); Mass: $[M+H]^+$; *m/z* 288.31; Elemental analysis: $C_{16}H_{20}N_2OS$. Calcd. formula weight 288.407; C, 66.5%; H, 6.9%; N, 9.7%; S, 11.1%.

4-(3-Nitrophenyl)-3,4,5,6,7,8,9-hexahydro-1*H*-cyclohepta[*d*]pyrimidine-2(5*H*)-thione (4c): Yield: 86%; m.p.: 276-277 ºC; Physical state/colour: Solid/pale yellow; IR (KBr, ν_{max}, cm^{-1}): 1615 (C=N *str.*), 1085 (C-N bend), 3167 (N-H *str.*), 1197 (C=S *str.*), 2940, 2854 (Ar C-H *str.*), 704, 774 (Ar C-H bend), 1493 (Ar C-C *str.*), 1615 (C=C *str.* alkene), 1001 (C-H bend, alkene), 3167 (C-H *str.*, alkene), 1535, 1354 (N-O *str.*, nitro); ^{1}H NMR: δ ppm: 2.1 (2H, t), 1.59-1.63 (2H, m), 3.75 (1H, d), 6.87 (1H, d), 7.04 (1H, s), 8.15 (m, *J* = 2.46 Hz), 7.45 (m, *J* = 7.75), 7.55 (m, *J* = 7.55 Hz); Mass: $[M+H]^+$; *m/z* 303.31; Elemental analysis: $C_{15}H_{17}N_3O_2S$. Calcd formula weight 303.379; C, 59.3%; H, 5.6%; N, 13.8%; S, 10.5%.

4-(5-Methoxynaphthyl)-3,4,5,6,7,8,9-hexahydro-1*H*-cyclohepta[*d*]pyrimidine-2(5*H*)-thione (4d): Yield: 79%; m.p.: 246-247 ºC; Physical state/colour: Solid/light brown; IR (KBr, ν_{max}, cm^{-1}): 1615 (C=N *str.*), 1085 (C-N bend), 3167 (N-H *str.*), 1197 (C=S *str.*), 2940, 2854 (Ar C-H *str.*), 704, 774 (Ar C-H bend), 1493 (Ar C-C *str.*), 1615 (C=C *str.* alkene), 1001 (C-H bend, alkene), 3167 (C-H *str.*, alkene), 1245 (C-O *str.*, -OMe), 1043 (C-O bend, -OMe); ^{1}H NMR: δ ppm: 2.1 (2H, t), 1.59-1.63 (2H, m), 3.61 (1H, d), 6.87 (1H, d), 7.04 (1H, s), 3.72 (methoxy proton, s), 6.81-7.15 (m, Ar-H, *J* = 2.3 Hz); Mass: $[M+H]^+$; *m/z* 337.89; Elemental analysis: $C_{20}H_{22}N_2OS$. Calcd. formula weight 338.466; C, 70.9%; H, 6.4%; N, 8.2%; S, 9.4%.

4-(4-Fluorophenyl)-3,4,5,6,7,8,9-hexahydro-1*H*-cyclohepta[*d*]pyrimidine-2(5*H*)-thione (4e): Yield: 87%; m.p.: 270-271 ºC; Physical state/colour: Solid/pale yellow; IR (KBr, ν_{max}, cm^{-1}): 1615 (C=N *str.*), 1085 (C-N bend), 3167 (N-H *str.*), 1197 (C=S *str.*), 2940, 2854 (Ar C-H *str.*), 704, 774 (Ar C-H bend), 1493 (Ar C-C *str.*), 1615 (C=C *str.* alkene), 1001 (C-H bend, alkene), 3167 (C-H *str.*, alkene), 1161-1236 (C-F *str.*, high intense); ^{1}H NMR: δ ppm: 2.1 (2H, t), 1.59-1.63 (2H, m), 3.75 (1H, d), 6.87 (1H, d), 7.04 (1H, s), 7.03-7.31 (m, *J* = 6.95 Hz); Mass: $[M+H]^+$; *m/z* 275.92; Elemental analysis: $C_{15}H_{17}FN_2S$. Calcd formula weight 276.372; C, 65.1%; H, 6.1%; N, 10.1%; S, 11.5%.

Antibacterial activity: The antibacterial activities of all the synthesized compounds (**4a-e**) were studied against Gram-positive bacteria (*S. aureus* and *Bacillus subtilis*) and Gram-negative bacteria (*E. coli* and *Klebsiella promioe*) at a concentration of 0.125 µg/mL by agar cup plate method [28]. A methanol system was used as control in this method. Under similar conditions, *ampicillin* was used as a standard control for comparison.

RESULTS AND DISCUSSION

XRD analysis: The XRD spectra of $FeTiO_3$ nanoparticles is represented in Fig. 1. It was observed that three characteristic peaks of ilmenite form of $FeTiO_3$ was formed at 2θ = 32º, 35º and 53º positions correspond to the diffraction planes (104), (110) and (116), respectively. These diffraction peaks indicates the formation of hexagonal structure with rhombic cell parameters of *a* = 5.087 and *c* = 14.10 Å (JCPDS card no. 79-1838) [25]. The other diffraction peaks obtained locates the remaining planes of $FeTiO_3$ in its non-stoichiometric ortho-rhombic form, $[Fe_{0.13}Ti_{0.81}]O_{1.92}$ with the lattice parameters *a* = 4.615, *b* = 51.35 and *c* = 2.95 Å (JCPDS card no.84-1595) [25]. In addition, it can be observed that the peak intensity has increased with increase in the content of Ti^{4+} ions in the nanoparticles, which shows the concentration of Ti^{4+} ions was retained in the synthesized nanoparticles at par with the combination ratio of the precursors used in their synthesis.

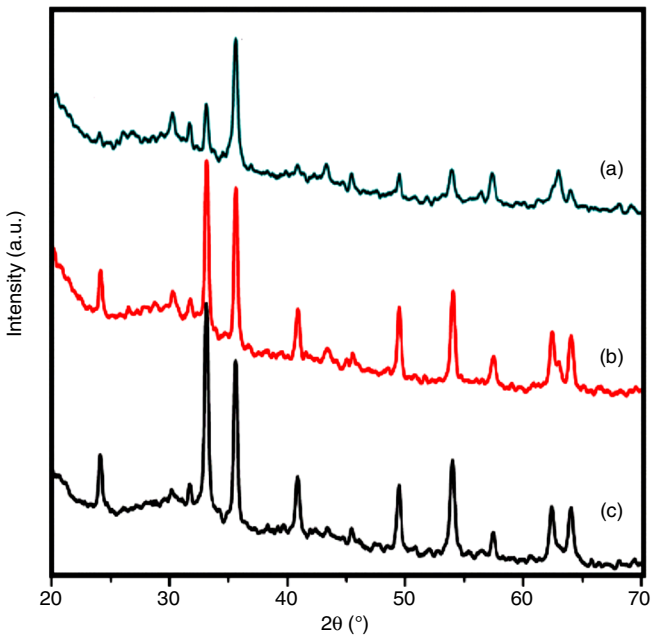

Fig. 1. XRD spectra of $FeTiO_3$ NPs. (a) TiFe-0.5; (b) TiFe-1.0; (c) TiFe-2.0

The average crystallite size of all the nanoparticles was calculated from Debye-Scherrer's equation [26] (eqn. 1) from FWHM (full width at half maximum) for the ilumenite indicator peaks.

$$D = \frac{K\lambda}{\beta\cos\theta} \quad (1)$$

where K is a dimensionless factor (0.9); λ is the X-ray wavelength (1.54059 Å); β is full width at half maxima (FWHM = 0.98072) and θ is the diffraction angle. From the Table-1, it is observed that all the catalysts were formed in nanoscale with a slight increase in the crystallite size on increasing the concentration of Ti^{4+} ions.

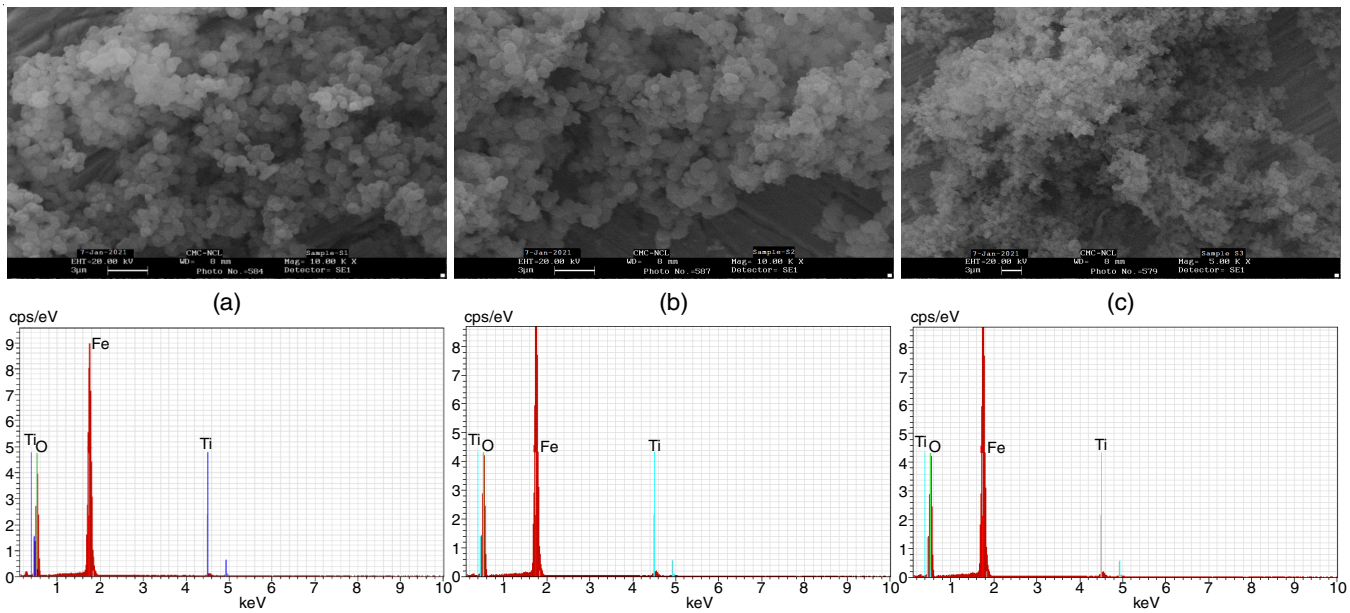

Fig. 2. FESEM image and EDAX spectra of (a) TiFe-0.5 NPs, (b) TiFe-1.0 NPs and (c) TiFe-2.0 NPs

TABLE-1
AVERAGE CRYSTALLITE SIZE OF $FeTiO_3$ NANOPARTICLES

Nanocatalysts	Average crystallite size, D (nm)
TiFe-0.5	22.12
TiFe-1.0	23.41
TiFe-2.0	25.18

FESEM-EDAX analysis: The morphology studies revealed the formation of spherical shaped nanoparticles in all the three combinations of $FeTiO_3$ (Fig. 2a-c). Also, with increase in the concentration of Ti^{4+} ions, there was no much difference in the morphology. The EDAX elemental analysis have shown the presence of all the respective atoms (Fe, Ti, O) in all the combinations.

UV-vis DRS analysis: In UV-vis DRS spectral analysis, all the three combinations of $FeTiO_3$ nanoparticle have shown a broad range of absorption between 380-570 nm (Fig. 3) indicating their suitability as catalysts in the visible region. In all the nanoparticles, a uniform maximum absorbance was noticed at around 400 nm with increasing absorbance capacity on increasing the composition of Ti^{4+} ions. Using eqn. 2 [26], the band gap was calculated in the range of 380 to 570 nm (maximum absorption range) and it was obtained between 3.26 to 2.17 eV.

$$E_g = \frac{1240}{\lambda} \quad (2)$$

where E_g is the band gap energy in electron volts and λ is the wavelength in nanometers.

Investigation of experimental factors for synthesizing derivatives 4a-e and their optimization: In order to optimize certain experimental factors that influence the formation of pyridimine-2-thione derivatives (**4a-e**) in better yields. To understand the effectiveness of the three different nanoparticles in bringing out the target derivatives in better yields, the experiment was conducted and the results are displayed in Table-2.

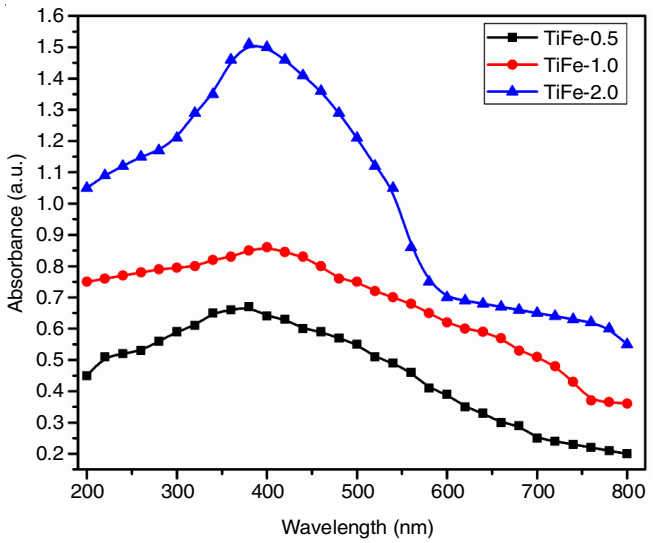

Fig. 3. UV-vis DRS spectra of $FeTiO_3$ NPs

TABLE-2
COMPARISON OF YIELD (%) OF COMPOUNDS **4a-e** OBTAINED WITH $TiFeO_3$ NANOPARTICLES

Nanocatalyst (5 mol %)	Yield (%)				
	4a	**4b**	**4c**	**4d**	**4e**
TiFe-0.5	73	74	75	69	79
TiFe-1.0	79	81	80	74	82
TiFe-2.0	83	88	86	79	87

It was noticed that with increase in the content of Ti in the nanoparticles, the % yield have increased and the TiFe-2.0 nanoparticles have formed the highest possible yields with good purity. Using the same nanoparticles, next step was conducted to find the role of its composition and the results are presented in Table-3. The $FeTiO_3$ nanoparticles with 5 mol % composition have shown the best performance among the chosen compositions. By using these factors, the influence of solvent

TABLE-3
EFFECT OF CATALYST COMPOSITION
FOR FORMATION OF COMPOUNDS **4a-e**

$FeTiO_3$ NPs (2.0 mL of TIP) (mol %)	Max. reflux time (h)	Average % yield of compounds **4a-e**
2.0	4	52
5.0	4	85
10.0	6	72
15.0	8	66
20.0	9	56

in forming the derivatives was performed with some selective solvents like ethanol, DMF, DMSO, glycerol, ethylene glycol and in water conditions (neat). It can observed from Table-4, that the reaction has shown the best yields under solvent free conditions and also the refluxing time was less with all the solvents except with neat. However, the % yields were found to be less with these solvents than with neat (%). In green chemistry scenario, recoverable and harmless solvents were given more importance [27] and hence, the present reaction scheme was found to be effective in the presence of neat (water). In the next series of experiments, the above optimized conditions were implemented to study the effect of refluxing time and reaction temperature and the results are showcased in Tables 5 and 6, respectively. The refluxing time varied from 1-5 h and

TABLE-4
EFFECT OF THE SOLVENT FOR
FORMATION OF COMPOUNDS **4a-e**

Solvent	Max. reflux time (h)	Average yield (%)[a]
Ethanol	1.5	65
DMF	1.0	71
DMSO	1.0	74
Glycerol	1.0	69
Ethylene glycol	1.0	76
Neat	4.0	85

Catalyst= TiFe-2.0 (5 mol %); Solvent = neat.
[a]Average % yield was calculated for the compounds **4a-e**.

TABLE-5
EFFECT OF TIME OF REFLUX FOR
FORMATION OF COMPOUNDS **4a-e**

Time of reflux (h)	Average yield (%)[a]
1	65
2	70
3	76
4	85
5	80

Reaction conditions: Catalyst: TiFe-2.0 (5 mol%); Solvent: neat.
[a]Average % yield was calculated for the compounds **4a-e**.

TABLE-6
EFFECT OF TEMPERATURE FOR
FORMATION OF COMPOUNDS **4a-e**

Temperature (°C)	Average yield (%)[a]
30-40	68
40-50	72
50-60	85
60-70	79
70-80	76

Reaction conditions: Catalyst: TiFe-2.0 (5 mol %). Solvent: neat. [a]Average % yield was calculated for the compounds **4a-e**. Reflux time: 4 h.

and found that for 4 h of refluxing, the average yield (%) of the compounds **4a-e** was found to be maximum. These results were obtained feasibly at 50-60 ºC, whereas at other selected temperatures, the fluctuating yields obtained.

Along with the above studies, the effectiveness of $FeTiO_3$ nanoparticles in forming the compounds **4a-e** in greater yields and solvent free conditions, the reaction was also conducted in the presence of few metal ferrites, $M^{II}Fe_2O_4$ (M = Cu, Ni, Zn and Co) under the established conditions. The results are shown in Table-7 and it can be observed that all the metal ferrites have produced the compounds with moderate yields, whereas the yields were higher with the $FeTiO_3$ nanoparticles (TiFe-2.0). This shows the importance of these nanoparticles towards synthesizing different organic derivatives under ambient conditions.

TABLE-7
CATALYTIC EFFECTIVENESS OF $FeTiO_3$
NANOPARTICLES THAN SOME SELECTED

Catalyst	Average % yield of compounds **4a-e**
$CuFe_2O_4$	73
$NiFe_2O_4$	77
$ZnFe_2O_4$	75
$CoFe_2O_4$	72
$FeTiO_3$	85

Reaction conditions: Catalyst: $M^{II}Fe_2O_4$ (5 mol%); TiFe-2.0 (5 mol%). Solvent: neat. [a]Average % yield was calculated for the compounds **4a-e**. Reflux time: 4 h; Temperature: 50-60 °C. [$M^{II}Fe_2O_4$ (M = Cu, Ni, Zn, Co)]

Recyclability of nanocatalyst: The effect of recyclability of the catalyst (TiFe-2.0) was conducted which was separated with a magnet. Using this recycled form and the optimized conditions, the synthesis of compounds (**4a-e**) was conducted 3 consecutive runs, by recycling the catalyst in each run. The recycled nanoparticles were washed with EtOH:water mixture thoroughly, dried and then used in further runs. The % yields of the compounds obtained is presented in Table-8. It was observed that in 2nd and 3rd runs the % yields were slightly nearer to that obtained in the 1st run (except compound **4d**). Whereas in the 4th run, the % yields have slightly decreased when compared with the previous runs and hence, it was analyzed that the reusability of the synthesized iron titanate nanoparticles was efficient up to two consecutive runs after the 1st run with the pure form of the nanoparticles.

TABLE-8
RECYCLABILITY OF THE NANOCATALYST (TiFe-2.0)
TOWARDS FORMATION OF COMPOUNDS **4a-e**

Cycle	Yield (%)				
	4a	**4b**	**4c**	**4d**	**4e**
1st run	70	68	70	69	67
2nd run (1st recycle)	68.5	66	68	66	66
3rd run (2nd recycle)	67	65	67	65	64
4th run (3rd recycle)	65	63	65	65	64

Antibacterial activity: It can be observed that compounds **4a**. **4b** and **4e** have shown good antibacterial activity against all the selected microorganisms, except on *K. pneumoniae*. Against this organism, compound **4b** (R = 4-methoxyphenyl)

has shown a moderate activity and the remaining compounds were almost less effective in deactivating it. Compounds **4a** (R = phenyl) and compound **4e** (R = 4-fluorophenyl) displayed good antibacterial activity whereas, compounds **4c** (3-nitrophenyl) and **4d** (5-methoxy napthyl) have shown less to moderate activity (Table-9). From these studies, it can be concluded that the groups phenyl, 4-methoxyphenyl and 4-fluorophenyl groups substituted on the moiety of the pyrimidine-2-thione have created improved antibacterial activity. In addition, the presence sulphur in this scaffold, might have also contributed for this biological feature.

TABLE-9
ANTIBACTERIAL ACTIVITY OF COMPOUNDS **4a-e**

Compounds	Zones of inhibition (diameter in mm), 0.125 µg/mL			
	Gram-positive		Gram-negative	
	SA	BS	KP	EC
4a	17	19	31	18
4b	17	18	25	15
4c	20	32	27	23
4d	23	29	33	31
4e	15	19	27	15
Ampicillin	28	36	35	37

SA = *Staphylococcus aurues*; BS = *Bacillus subtilis*; KP = *Klebsiella Pneumoniae*; EC = *Escherichia coli*

Conclusion

Present work presents a green one-pot synthesis of pyrimidine-2-thione derivatives (**4a-e**) using $FeTiO_3$ nanoparticles (5 mol%) and solvent free conditions. The characterization results of the nanocatalysts and the synthesized organic derivatives have shown satisfactory results. The major outcome of this reaction is that the derivatives were synthesized with $FeTiO_3$ nanoparticles (ilmenite) unlike its ulvospinel form, $TiFe_2O_4$, which was noticed as first of its kind. The derivatives (**4a-e**) were investigated for antibacterial activity and it was observed that three compounds (**4a**, **4b** and **4e**) have displayed moderate and good activity. Therefore, it can be concluded that the established scientific method was novel and facile in its own way.

ACKNOWLEDGEMENTS

One of the authors, Rambabu, is thankful to Advanced Analytical Laboratory, Andhra University, Visakhapatnam, India for providing the spectral analysis.

CONFLICT OF INTEREST

The authors declare that there is no conflict of interests regarding the publication of this article.

REFERENCES

1. C.D. Cox, M.J. Breslin and B.J. Mariano, *Tetrahedron Lett.*, **45**, 1489 (2004); https://doi.org/10.1016/j.tetlet.2003.12.026
2. B.K. Karale, C.H. Gill, M. Khan, V.P. Chavan, A.S. Mane and M.S. Shingare, *Indian J. Chem.*, **41B**, 1957 (2002).
3. M.A. El-Hashash, M.R. Mahmoud and S.A. Madboli, *Indian J. Chem.*, **32B**, 449 (1993).
4. D.J. Brown, The Chemistry of Heterocyclic Compounds, The Pyrimidines, Vol. 52, Wiley: New York, USA (1994).
5. M. Kidwai and M. Mishra, *J. Serb. Chem. Soc.*, **69**, 247 (2004); https://doi.org/10.2298/JSC0404247K
6. D.J. Brown, Eds.: A.J. Boulton and A. McKillop, Comprehensive Heterocyclic Chemistry, Pergamon: Oxford, UK, vol. 3, p. 150 (1984).
7. C.O. Kappe, *Tetrahedron*, **49**, 6937 (1993); https://doi.org/10.1016/S0040-4020(01)87971-0
8. A. Dondoni, A. Massi and S. Sabbatini, *Tetrahedron Lett.*, **43**, 5913 (2002); https://doi.org/10.1016/S0040-4039(02)01269-8
9. C. Ramalingan and Y. Kwak, *Tetrahedron*, **64**, 5023 (2008); https://doi.org/10.1016/j.tet.2008.03.078
10. S.M. Sondhi, R.N. Goyal, A.M. Lahoti, N. Singh, R. Shukla and R. Raghubir, *Bioorg. Med. Chem.*, **13**, 3185 (2005); https://doi.org/10.1016/j.bmc.2005.02.047
11. M. Movassaghi and M.D. Hill, *J. Am. Chem. Soc.*, **128**, 14254 (2006); https://doi.org/10.1021/ja066405m
12. J. Safaei-Ghomi and A. Ghasemzadeh, *J. Serb. Chem. Soc.*, **76**, 679 (2011); https://doi.org/10.2298/JSC100212057S
13. X. Yang, X. Wang and Z. Zhang, *J. Cryst. Growth*, **277**, 467 (2005); https://doi.org/10.1016/j.jcrysgro.2005.02.004
14. J.A. Gomes, M.H. Sousa, F.A. Tourinho, J. Mestnik-Filho, R. Itri and J. Depeyrot, *J. Magn. Magn. Mater.*, **289**, 184 (2005); https://doi.org/10.1016/j.jmmm.2004.11.053
15. A.T. Raghavender, R.G. Kulkarni and K.M. Jadhav, *Zhongguo Wuli Xuekan*, **46**, 366 (2008).
16. N. Iftimie, E. Rezlescu, P.D. Popa and N. Rezlescu, *J. Optoelectron. Adv. Mater.*, **8**, 1016 (2006).
17. L. Satyanarayana, K.M. Reddy and S.V. Manorama, *Mater. Chem. Phys.*, **82**, 21 (2003); https://doi.org/10.1016/S0254-0584(03)00170-6
18. Z. Tianshu, P. Hing, Z. Jiancheng and K. Lingbing, *Mater. Chem. Phys.*, **61**, 192 (1999); https://doi.org/10.1016/S0254-0584(99)00133-9
19. X. Chu, X. Liu, Y. Song and G. Meng, *Sens. Actuators B Chem.*, **61**, 19 (1999); https://doi.org/10.1016/S0925-4005(99)00269-5
20. V. Jeseentharani, M. George, B. Jeyaraj, A. Dayalan and K.S. Nagaraja, *J. Exp. Nanosci.*, **8**, 358 (2013); https://doi.org/10.1080/17458080.2012.690893
21. A. Shukla, A.K. Bhardwaj, B.K. Pandey, S.C. Singh, K.N. Uttam, J. Shah, R.K. Kotnala and R. Gopal, *J. Mater. Sci. Mater. Electron.*, **28**, 15380 (2017); https://doi.org/10.1007/s10854-017-7423-3
22. A. Shukla, A.K. Bhardwaj, S.C. Singh, K.N. Uttam, N. Gautam, A.K. Himanshu, J. Shah, R.K. Kotnala and R. Gopal, *J. Appl. Phys.*, **123**, 161411 (2018); https://doi.org/10.1063/1.5008733
23. D.H. Dawood, E.M.H. Abbas, T.A. Farghaly, M.M. Ali and M.F. Ibrahim, *Med. Chem.*, **15**, 277 (2019); https://doi.org/10.2174/1573406414666180912113226
24. A.M. Mudarra Navarro, A.V. Gil Rebaza, K.L. Salcedo Rodriguez, J.J. Melo Quintero, C.E. Rodriguez Torres, M. Weissmann and L.A. Errico, *J. Phys. Chem. C*, **123**, 21694 (2019); https://doi.org/10.1021/acs.jpcc.9b06550
25. R.A.P. Ribeiro and S.R. de Lazaro, *RSC Adv.*, **4**, 59839 (2014); https://doi.org/10.1039/C4RA11320A
26. A.V. Prasada Rao, A.M. Umabala and P. Suresh, *J. Applicable Chem.*, **4**, 1145 (2015).
27. B.A. de Marco, B.S. Rechelo, E.G. Totoli, A.C. Kogawa and H.R.N. Salgado, *Saudi Pharm. J.*, **27**, 1 (2019); https://doi.org/10.1016/j.jsps.2018.07.011
28. R.S. Hiremath and H.S. Shubha, *J. Res. Ayurveda*, **31**, 260 (2010); https://doi.org/10.4103/0974-8520.72412